Dalton Transactions

Cite this: *Dalton Trans.*, 2012, **41**, 3239

www.rsc.org/dalton

PAPER

Lanthanide-binding peptides with two pendant aminodiacetate arms: Impact of the sequence on chelation†

Agnieszka Niedźwiecka,[a] Federico Cisnetti,[a,b] Colette Lebrun,[a] Christelle Gateau[a] and Pascale Delangle*[a]

Received 6th September 2011, Accepted 21st December 2011
DOI: 10.1039/c2dt11686c

Lanthanide complexes with a series of hexapeptides—incorporating two unnatural chelating amino acids with aminodiacetate groups, Ada_1 and Ada_2—have been examined in terms of their speciation, structure, stability and luminescence properties. Whereas Ada_2 acts as a tridentate donor in all cases, Ada_1 may act as a tetradentate donor thanks to the coordination of the amide carbonyl function assisted by the formation of a six-membered chelate ring. The position of the Ada_1 residue in the sequence is demonstrated to be critical for the lanthanide complex speciation and structure. Ada_1 promotes the coordination of the backbone amide function to afford a highly dehydrated Ln complex and an S-shape structure of the peptide backbone, only when found in position 2.

Introduction

Metal-binding peptides or pseudopeptides are interesting candidates as models of biological metal transporters,[1] efficient toxic metal chelators[2] or to design metal-based probes.[3,4] In particular, the application of the unique magnetic and spectroscopic properties of trivalent lanthanide ions (Ln^{3+})[5] to magnetic resonance imaging[6] and optical imaging of cells[7] is of increasing interest. Therefore, Ln-peptide complexes have been investigated by several research groups to benefit both from Ln-based spectroscopic properties and the biological peptide scaffold. Ln-complexing peptides or proteins have been elaborated *de novo*[4] or starting from naturally occurring Ca^{2+} binding loops as Ca^{2+} and Ln^{3+} have similar ionic radii.[8,9] Lanthanide Binding Tags (LBT) developed by B. Imperiali's group are short peptides optimized for tight Ln^{3+} binding and water exclusion from the coordination sphere in order to obtain efficient sensitized terbium luminescence.[10,11] These LBTs have been coupled to proteins to investigate their structure, function and dynamics by X-ray crystallography, paramagnetic induced NMR data, or Ln-luminescence-based techniques.[3] However, the above-mentioned examples show that there is an intrinsic limitation of the stability of lanthanide-peptide complexes if only natural amino acids are used. Indeed, the latter bear only simple binding groups like carboxylates (Asp, Glu), phenolates (Tyr), or amides (Asn, Gln, backbone peptide linkage) which have low affinity for Ln^{3+} in comparison to synthetic multidentate ligands of the poly(aminocarboxylate) family.

Peptides containing unnatural chelating amino acids were recently designed in our group to obtain Ln-binding peptides of enhanced stability with a ligating site embedded in the peptide framework.[12,13] Two synthetic amino acids, which bear tridentate aminodiacetate chelating groups (Ada_n) were introduced in short peptide sequences to obtain **P^{11}**, **P^{22}** and **P^{33}** (Scheme 1). These compounds may be viewed as models of polyaminocarboxylate ligands, namely EDTA or TMDTA, with a peptide spacer instead of an alkyl chain. In such systems, the peptide backbone is used as a non-innocent spacer between the coordinating groups and a central Pro-Gly unit was chosen to favour the formation of a β-turn containing structure.[14]

We have shown that the length of the alkyl chain between the main peptide backbone and the aminodiacetate moiety (1, 2 or 3 methylene units) has a marked effect on both the stability and structure of the complexes. The most flexible peptide **P^{33}** forms low stability complexes in which the two aminodiacetate moieties tend to act as independent chelating groups. Interestingly, the peptide **P^{22}** provides exclusively a stable mononuclear Ln complex ($\beta_{110} = 10^{12.1}$) with a triply hydrated Tb^{3+} ion.[12] The use of shorter alkyl chains in **P^{11}** seemed very promising to us as they favour the coordination of a backbone carbonyl due to the formation of a six-membered chelate ring and afford higher

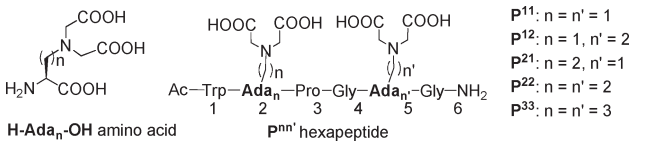

Scheme 1 Design of lanthanide-binding peptides incorporating Ada_n residues.

[a]*INAC, Service de Chimie Inorganique et Biologique (UMR_E 3 CEA UJF), Commissariat à l'Energie Atomique, 17 Rue des Martyrs, 38054 Grenoble Cedex, France. E-mail: pascale.delangle@cea.fr; Fax: +33 4 3878 5090; Tel: +33 4 3878 9822*
[b]*Present address: Clermont Université, Université Blaise Pascal, Laboratoire SEESIB, UMR CNRS 6504, 24 Avenue des Landais, 63177 Aubière Cedex, France*

†Electronic supplementary information (ESI) available: pH-metric titrations, isotope patterns of polymetallic complexes, fluorescence of Trp, fluorescence titrations with $EuCl_3$, determination of luminescence lifetimes, competitive titration with $TbCl_3$, NMR tables. See DOI: 10.1039/c2dt11686c

denticity. This induces a lower hydration state of the Tb^{3+} ion in the complex.[13] These differences in the Ln^{3+} ion coordination by **P11** and **P22** modify profoundly the structures of the peptides as revealed by the solution NMR structures of the two complexes La**P22** and Lu**P11**. In La**P22**, the Ada_2PGAda_2 motif forms a type II β-turn and the peptide backbone adopts a U-shape structure with the La^{3+} ion located above the peptide backbone plane. On the contrary, Lu**P11** revealed an extended S-shape structure due to the extra coordination of the amide carbonyl of $Ada_1(2)$, which prevents the formation of the β-turn and drives the Ln^{3+} ion in the proline plane and closer to the Trp indole sensitizer (Fig. 1).

In this article, we report the synthesis and Ln complexation properties of two novel hexapeptides **P12** and **P21** which contain one Ada_1 and one Ada_2 non natural chelating amino acids. These two peptides were expected to exhibit intermediate properties between **P22** and **P11**. We demonstrate that the position of the Ada_1 residue in the sequence is critical for the Ln complex speciation and structure. The spectroscopic properties of the Ln complexes with the series of $\mathbf{P^{nn'}}$ peptides (**n,n′** = 1,2) demonstrate that **P12** forms a mononuclear complex similar to Ln**P11** without the drawback of polymetallic complexes formation. On the contrary, **P21** behaves like **P22** with Ada_1 inducing a more complicated speciation. The position of the chelating amino acid Ada_1 in the peptide sequence is therefore critical to promote the coordination of the backbone carbonyl which leads to dehydrated Ln complexes.

Results and discussion

1. Synthesis of Ada_1 containing peptides P11, P12 and P21

The synthesis of small peptides incorporating unnatural amino acids (Ada_n) bearing aminodiacetate groups was performed by solid phase peptide synthesis (SPPS) using standard Fmoc/*t*Bu strategy.

The synthon Fmoc-Ada_2(*t*Bu)$_2$-OH, which is directly used in the SSPS, was previously prepared in good yield starting from commercially available N^{α}-Fmoc protected amino acid derivatives.[12] The synthesis of the protected N^{α}-Fmoc-Ada_1(*t*Bu)$_2$-OH amino acid is described in Scheme 2. The latter compound was prepared following a method adapted from Kazmierski[15] as performed previously for the synthesis of Fmoc-Ada_3(*t*Bu)$_2$-OH.[12] Commercial N^{α}-Fmoc and N^{β}-Boc protected L-diaminopropionic acid, Fmoc-Dpr(Boc)-OH, **1**, was benzylated using a published procedure[16] to obtain compound **2** in 82% yield. Then, the Boc

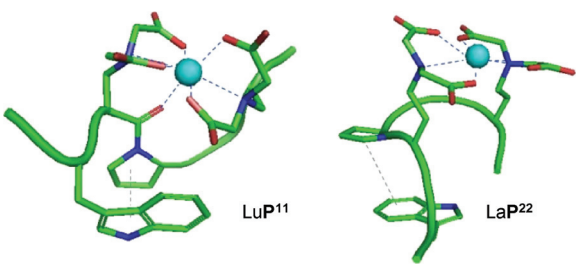

Fig. 1 NMR solution structures (lowest energy) of Lu**P11** and La**P22**, evidencing the S-shape and U-shape of the backbones, respectively.[12,13]

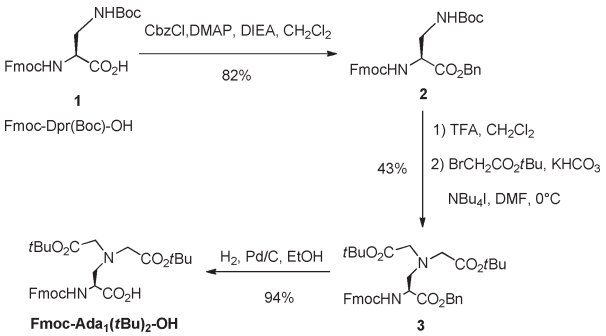

Scheme 2 Synthesis of Fmoc-Ada_1(*t*Bu)$_2$-OH.

protection was removed in a strong acid medium and the resulting amine was alkylated with $BrCH_2CO_2tBu$ at 0 °C to afford compound **3** in 43% yield over two steps. Conducting this reaction at higher temperature resulted in lower yields due to Fmoc deprotection. The final Fmoc-Ada_1(*t*Bu)$_2$-OH was recovered after hydrogenolytic debenzylation. The coupling of Fmoc-Ada_1(*t*Bu)$_2$-OH with a chiral amine (α-methylbenzylamine) either in an enantiopure or a racemic form allowed us to prove the enantiomeric purity of the latter compound. Indeed, the coupling products were examined by ^{1}H NMR and splitting of some signals (especially NH doublets) occurred only in the coupling product with the racemic amine, indicating that the Fmoc-Ada_1(*t*Bu)$_2$-OH synthon was enantiopure.

Peptides **P11**, **P12** and **P21** (Scheme 1) were then manually assembled by solid phase peptide synthesis (SSPS) starting from Fmoc-Ada_n(*t*Bu)$_2$-OH and natural commercial amino acid derivatives, on Rink amide MBHA resin using standard conditions as performed previously for **P22**.[12] No significant by-products were detected, showing that the unnatural amino acid Fmoc-Ada_1(*t*Bu)$_2$-OH displayed normal reactivity in the on-resin synthetic steps as the two longer chains analogues Ada_2 and Ada_3. Before resin cleavage, N-terminal acetylation was performed. As the choice of the resin ensured the isolation of peptides as *C*-terminal amides, peptides were recovered after simultaneous resin cleavage and side-chain deprotection with both extremities protected. The pure peptides were obtained in a 50 mg scale after preparative HPLC purification. The identity and purity of the peptides were confirmed by electrospray ionization mass spectrometry and standard combination of 1D and 2D ^{1}H-NMR techniques.[17] ROESY spectra for both peptides (500 MHz, 298 K) showed no though-space correlations other that sequential ones. This, along with little dispersion of the NH-amide and glycine Hα resonances is indicative of flexible conformations in solution as expected for linear oligopeptides (Tables S1 to S3†).

2. Peptide protonation

The protonation states of Ada_n amino acids in the sequences affect the structure, the solubility and the metal-binding properties of the peptide scaffolds. Therefore, the acid/base properties of **P11** and **P21** were investigated with pH-metric titrations. Measured pK_as are reported in Table 1 (see Fig. S1 for titration curves†). Four pK_as were determined for each peptide: two pK_as (> 6) correspond to the ammonium functions and two pK_as (< 4)

Table 1 Equilibrium constants of $\mathbf{P^{nn'}}$ peptides and $\mathbf{LnP^{nn'}}$ complexes[a]

Equilibrium constants in water solution of **L**	$\mathbf{P^{11}}$	$\mathbf{P^{12}}$	$\mathbf{P^{21}}$	$\mathbf{P^{22}}$[b]
pK_{a1}	7.2(1)		8.4(1)	8.8(1)
pK_{a2}	6.4(1)		6.2(1)	8.2(1)
pK_{a3}	3.0(1)		2.8(1)	2.8(1)
pK_{a4}	~2		~2	~2
$\log\beta_{110}^{pH=7}$ (Tb**L**)	10.3(5)[c]	9.5(5)	9.0(5)	9.1(5)
$\log\beta_{110}$ (Tb**L**)	10.8(5)	11.0(5)[d]	10.5(5)	12.1(5)

[a] The experiments were performed at ionic strength I = 0.1 M (KCl) at 25 °C. $\log\beta_{110}^{pH=7}$ are the conditional stability constants at pH = 7.0 and $\log\beta_{110}$ are the global stability constants; [b] From reference 12. [c] From reference 13. [d] Calculated, assuming that the pK_a values for $\mathbf{P^{12}}$ and $\mathbf{P^{21}}$ are the same.

are assigned to carboxylic functions. Not all carboxylic acids (pK_{a5} and pK_{a6} are < 2) could be detected due to sample dilution. The values of pK_{a1} and pK_{a2} are essential for the calculation of the stability constants from the measured conditional values at pH = 7.0, as described later in this paper.

The first pK_a of $\mathbf{P^{11}}$ corresponds to the deprotonation of Ada_1 ammonium function. Therefore its value is lower than the value obtained with $\mathbf{P^{22}}$,[12] due to the larger withdrawing effect of the peptide backbone amide functions through the short side-chains of Ada_1 in $\mathbf{P^{11}}$. As expected, the first pK_a of $\mathbf{P^{21}}$ is in the same range as for $\mathbf{P^{22}}$ because both correspond to the deprotonation of the ammonium group of an Ada_2 residue. In summary, the three peptide basicities follow the order: $\mathbf{P^{22}} > \mathbf{P^{21}} > \mathbf{P^{11}}$. Moreover, it is expected that $\mathbf{P^{12}}$ and $\mathbf{P^{21}}$ display a similar behaviour towards protonation as these two peptides do not show specific secondary structures that could affect the pK_a values.

3. Formation and stability of $\mathbf{LnP^{nn'}}$ complexes

A tryptophan residue was inserted in the peptide sequence to enable the energy transfer from the indole moiety ($\lambda_{exc,max}^{Trp}$ = 280 nm) to the Tb^{3+}/Eu^{3+} ion coordinated in a close proximity. Thanks to the tryptophan sensitizer, lanthanide luminescence can be easily detected. The $\mathbf{LnP^{nn'}}$ complexes exhibit interesting spectroscopic characteristics, such as long-lived luminescence lifetimes, large Stokes shifts and sharp emission bands in the visible range. The titration of peptide solutions in HEPES buffer (10 mM, 0.1 M KCl, pH = 7.0) with Tb^{3+} show linear evolutions of Trp fluorescence ($\lambda_{em,max}^{Trp}$ = 350 nm) and gradual growths of $^5D_4 \rightarrow {}^7F_J$ bands (J = 3–6) of Tb luminescence, from 0 to 1 equiv. of metal added. These behaviours are consistent with the formation of a unique $\mathbf{TbP^{nn'}}$ complex, in excess of peptide (Fig. 2). A plateau is obtained after one Tb^{3+} equiv. with $\mathbf{P^{22}}$ and $\mathbf{P^{12}}$. However the signals still slightly evolve in the presence of excess $Tb^{3+}$with $\mathbf{P^{11}}$ and $\mathbf{P^{21}}$, due to the formation of other metal complexes.

Electrospray mass spectrometry (ES-MS) and circular dichroism (CD) confirmed these observations. Samples analyzed by ES-MS contained one $\mathbf{P^{nn'}}$ peptide and europium chloride in different proportions, in $AcONH_4$ buffer (20 mM, pH = 7.0). The spectra recorded in positive ionization mode are presented in Fig. 3. $\mathbf{P^{12}}$ complexation results exclusively in the

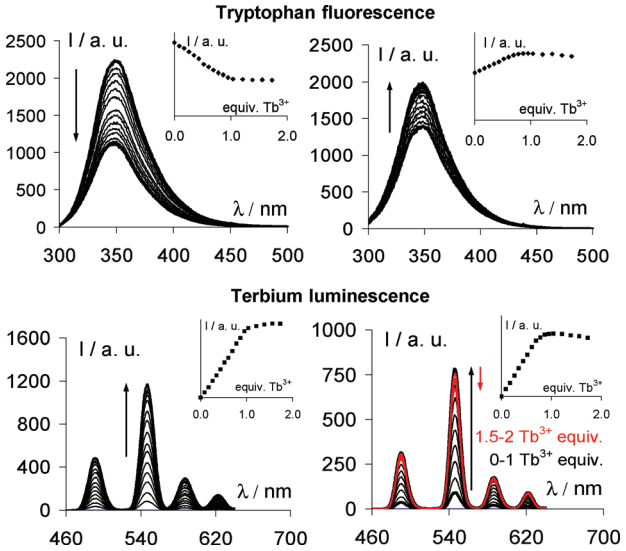

Fig. 2 Titrations of $\mathbf{P^{12}}$ (left) and $\mathbf{P^{21}}$ (right) (20 μM) with $TbCl_3$ in HEPES buffer (10 mM, pH 7). Evolution of tryptophan fluorescence and Tb-centred luminescence upon excitation at 280 nm (inserts: evolution of the luminescence intensity at λ_{max}).

monometallic europium complex ($\mathbf{EuP^{12}}$). On the contrary, $\mathbf{P^{21}}$ forms significant amounts of the polymetallic species $Eu_2\mathbf{P^{21}}$ and $Eu_3\mathbf{P^{21}}_2$ in excess of metal ion. The isotope patterns of these complexes match the theoretical isotope patterns as seen in Fig. S2.† Moreover, signals of the free peptide with 1 equiv. or excess of $EuCl_3$ are detected with $\mathbf{P^{21}}$ and not with $\mathbf{P^{12}}$. The ES-MS experiments point to a rather complicated speciation with the peptide $\mathbf{P^{21}}$ whereas $\mathbf{P^{12}}$ forms only the mononuclear europium complex. These behaviours were corroborated by circular dichroism measurements.

As described before, CD titrations of the peptide ligands with lanthanide ions are very sensitive to metal complexation. In particular, polymetallic complexes formed in excess of metal ion

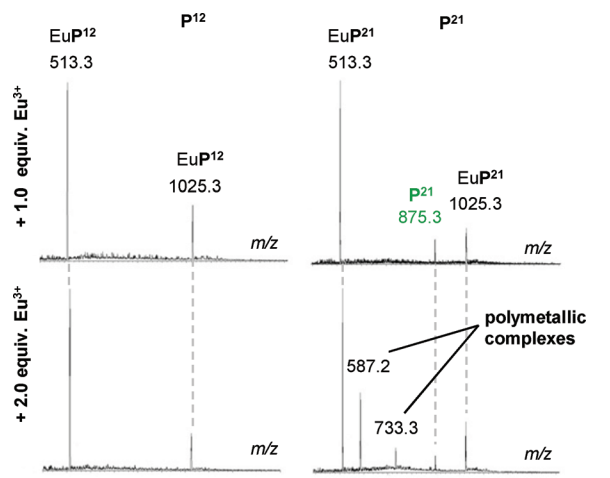

Fig. 3 ES^+-MS spectra of solutions containing $\mathbf{P^{12}}$ or $\mathbf{P^{21}}$ peptide (60 μM) and $EuCl_3$ (1 and 2 equiv.) in $AcONH_4$ buffer (20 mM, pH = 7.0). The less intense peaks of sodium and potassium adducts were removed for simplification. The signals at m/z = 587.2 and 733.3 correspond to the polymetallic complexes $Eu_2\mathbf{P^{21}}$ and $Eu_3\mathbf{P^{21}}_2$, respectively.

have significantly different CD signatures in comparison to monometallic complexes. Indeed the formation of the former leads to more elongated peptide structures in comparison with the mononuclear complexes with the two Ada_n coordinated to the same metal ion. Using such CD titrations, we previously demonstrated that **P^{11}** forms higher nuclearity complexes after one Ln^{3+} equiv.,[13] while **P^{22}** gave only a mononuclear complex, which does not transform in excess of metal ion.[12] The titrations of the peptides with Tb^{3+} show isodichroic points from 0 to 1 equiv. of added metal (**P^{11}**: 220 nm,[13] **P^{22}**: 208 nm,[12] **P^{12}**: 227 nm and **P^{21}**: 220 nm), which proves the formation of a unique complex (Fig. 4). After 1 Tb^{3+} equiv., the two compounds show different behaviours. CD spectra recorded with **P^{12}** do not evolve, which confirms the absence of polymetallic complexes. On the contrary, higher nuclearity complexes with a different CD signature (in red Fig. 4 bottom) are evidenced with **P^{21}**.

Overall, ES-MS, CD and luminescence titrations highlight the formation of polymetallic complexes with **P^{11}** and **P^{21}**, whereas **P^{22}** and **P^{12}** induce a simple speciation with the formation of a single mononuclear LnP complex.

The conditional stability constants of Tb**P$^{nn'}$** complexes at pH = 7.0, β_{11}^{pH7}, were determined by competition experiments between two peptides, which Tb complexes have significantly different time-resolved luminescence intensities. Such a competition, performed with peptide **P^{22}** as a reference of known affinity for Tb allowed us previously to obtain the affinity constant of Tb**P^{11}**.[13] Similar experiments were run to obtain Tb**P^{12}** and Tb**P^{21}** stabilities—values are reported in Table 1. Typical experiments are presented in Fig. S3 and S4.† The values of the conditional stability constants determined at a specific pH are dependent on the basicity of the ligands. Therefore, to compare the stabilities of the four Tb**P$^{nn'}$** complexes, the stability constants $\log\beta_{110}$ were calculated from the conditional constants at pH = 7.0 and the pK_as of the peptides. It appears that **P^{22}** forms the most stable Tb complex with a $\log\beta_{110}$ = 12.1. The three other complexes have $\log\beta_{110}$ values ranging from 10.5 to 11.0. This shows that the additional coordination of $Ada_1(2)$ carbonyl does not enhance the stabilities of Tb**P^{11}** and Tb**P^{12}**. Nevertheless, the latter complexes demonstrate higher stabilities at neutral pH, due to their lower overall basicity.

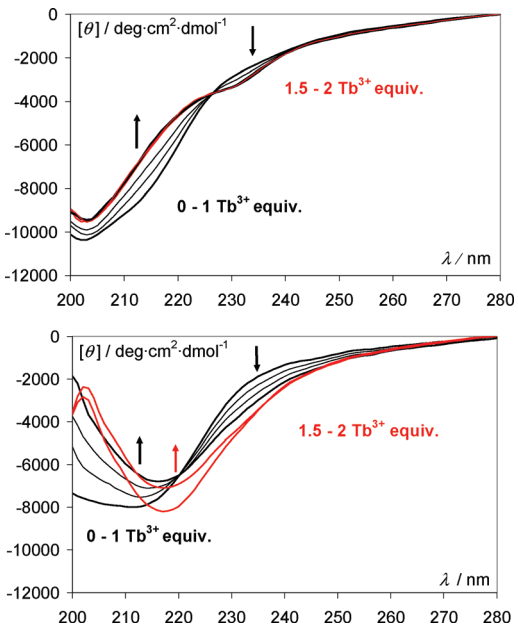

Fig. 4 Circular dichroism titration of 20 μM water solutions of **P^{12}** (top) and **P^{21}** (bottom) with $Tb(OTf)_3$ at pH = 7.0. Titration with 0.33 Tb equiv. until 1 equiv. (black curves) and 0.5 equiv. until 2 equiv (red curves).

4. Photophysical properties

Tryptophan fluorescence. The evolution of the tryptophan fluorescence shows interesting features that point to different behaviours of **P^{11}** and **P^{12}** in comparison to **P^{22}** and **P^{21}**. Several effects determine Trp fluorescence evolution upon Ln^{3+} binding: indole environment modification, energy transfer to the Ln^{3+} ion and in some cases photoinduced electron transfer. The comparison of Trp fluorescence of **P^{12}** with different Ln ions is shown as an example in Fig. S5.†

With Eu^{3+}, quenching of the Trp fluorescence is observed for the four peptides as a result of photoinduced electron transfer (PET).[18] Indeed this quenching mechanism has been demonstrated to highly contribute with Eu^{3+} and Yb^{3+}, the two most readily reduced Ln^{3+} ions.[19] For that reason, the four peptides show a 34% (**P^{22}**) to 81% (**P^{12}**) decrease of Trp luminescence upon Eu^{3+} addition, in comparison with the free peptide (Fig. S5 and S6†).

The indole environment modification upon complexation can be estimated by recording the fluorescence spectra of the free peptide and its La complex, since La^{3+} has no accessible energy levels for energy transfer and is not susceptible to PET. The spectra recorded with Tb^{3+} give exactly the same results as with La^{3+}, which demonstrates that the energy transfer from Trp to Tb^{3+} is undetectable, even though the latter ion is significantly sensitized upon binding to the peptides as seen in the time-resolved Tb^{3+} luminescence spectra shown in Fig. 2. Therefore, the evolution of Trp fluorescence during the titration with Tb^{3+} reflects only changes in the environment of the indole moiety upon Tb^{3+} complexation rather than a Trp → Tb^{3+} energy transfer.[12,20] The complexation of Tb^{3+} or La^{3+} by **P^{11}** and **P^{12}** induces a decrease of the Trp fluorescence of 40% and 52%, respectively. On the contrary, for **P^{22}** and **P^{21}** the Trp fluorescence increases of 40% and 26%, respectively. These data indicate that the indole environment, which is closely related to the peptide conformation, is similar for **P^{11}** and **P^{12}** Tb complexes on the one hand and for **P^{22}** and **P^{21}** on the other hand.

Luminescence lifetimes and hydration states. The luminescence lifetimes of Tb and Eu in the Ln**P$^{nn'}$** complexes in H_2O and D_2O solutions were measured in order to obtain the hydration number q of these complexed ions with the empirical equations by Parker *et al.*[21] To avoid underestimation of luminescence lifetimes in D_2O because peptides are accompanied by H_2O hydration molecules, τ_{D2O} was determined as the extrapolated limit of the luminescent decay rates in solutions of increasing D_2O molar fractions tending to an H_2O-free solution (Fig. S7†). The experimental values of τ_{H2O} and τ_{D2O} with the calculated hydration numbers are reported in Table 2. For Ln**P^{21}** and Ln**P^{22}**, hydration numbers close to 3 are in agreement with

Table 2 Luminescence lifetimes and calculated hydration numbers for Tb**P**$^{nn'}$ and Eu**P**$^{nn'}$ complexes

Complex	τ_{H2O}/ms	τ_{D2O}/ms	q
TbP^{11}[a]	2.00(2)	3.44(3)	0.7(1)
TbP^{12}	2.36(2)	3.13(3)	0.2(1)
TbP^{21}	1.09(1)	3.51(3)	2.9(1)
TbP^{22}[b]	1.11(1)	3.71(3)	2.9(1)
EuP^{11}	0.51(1)	1.34(1)	1.2(2)[c]
EuP^{12}	0.60(1)	1.54(1)	0.9(2)[c]
EuP^{21}	0.31(1)	1.98(2)	3.0(5)
EuP^{22}	0.30(1)	2.13(2)	3.1(5)

[a] Values from reference 13. [b] Values from reference 12. [c] Calculated without taking into account the quenching effect of individual amide N–H oscillators. Considering the quenching effect of one amide N–H oscillator (0.075 ms^{-1} contribution) gives q = 1.1 (Eu**P^{11}**) and 0.8 (Eu**P^{12}**).

both peptides behaving as hexadentate ligands like [Ln(EDTA)$(H_2O)_q$]$^-$ complexes.[21,22] On the contrary, longer luminescence lifetimes in H_2O are obtained for Ln**P^{12}** and Ln**P^{11}**, which exhibit much lower hydration numbers, inferior or close to 1. This can be related to the coordination of an extra donor group, as previously evidenced in the NMR solution structure of Lu**P^{11}**, which showed that the backbone carbonyl of Ada_1(2) was coordinated to the Lu^{3+} ion. These data demonstrate that the carbonyl group of the Ada_1 residue is able to coordinate the Ln^{3+} ion only if placed in position 2 in the hexapeptide sequence.

Quantum yields. The quantum yields of Ln**P$^{nn'}$** (Ln = Eu, Tb and **n,n′** = 1,2) were measured following the procedure of Bünzli *et al.*[23] In our case, the convenience of this protocol is the use of Eu and Tb tris(dipicolinates) as secondary standards, which excitation band ($\lambda_{exc,max}$ (Eu(dpa)$_3$/Tb(dpa)$_3$) = 279 nm) perfectly overlap with the excitation band of tryptophan ($\lambda_{exc,max}$ (Trp) = 280 nm). The values Φ_{tot}^{Tb} = 2–6 × 10^{-3} and Φ_{tot}^{Eu} = 1–2 × 10^{-3} are rather small as demonstrated in the literature for Eu^{3+} or Tb^{3+} sensitization by tryptophan.[9,20]

With Eu, the two important contributions to the overall quantum yield Φ_{tot}^{Eu}, *i.e.* the metal-centred visible light emission, Φ^{Eu}, and the sensitization efficiency, η_{sens}, can be evaluated (eqn (1)).[24–26]

$$\Phi_{tot}^{Eu} = \eta_{sens} \times \Phi^{Eu} \quad (1)$$

Indeed, the quantum yield Φ^{Eu} of the lanthanide luminescence step can be estimated from the observed metal ion lifetime in the complex and the radiative lifetime τ_R of the Eu($^5D_0$) level, given by eqn (2).[24–26]

$$\frac{1}{\tau_R} = A_{MD,0} n^3 \left(\frac{I_{tot}}{I_{MD}}\right) \quad (2)$$

Where n is the refractive index of the medium, $A_{MD,0}$ (= 14.65 s^{-1}) is the spontaneous emission probability for the $^5D_0 \rightarrow {}^7F_1$ transition and I_{tot}/I_{MD} is the ratio of the total area of the corrected Eu^{3+} emission spectrum to the area of the $^5D_0 \rightarrow {}^7F_1$ band.

This method was applied to Eu**P^{12}** which shows the most intense metal-centred emission spectrum. We experimentally measured I_{tot}/I_{MD} = 4.18 and calculated τ_R = 6.9 ms (n = 1.334 for water). The quantum yield of the lanthanide luminescence step can then be calculated Φ^{Eu} = 0.09. This figure is lower than values obtained with totally dehydrated complexes (q = 0)[26] due to the O–H vibrations of the coordinated water molecule in Eu**P^{12}**, which efficiently quench the Eu luminescence. However, monohydrated Eu complexes with macrocyclic DOTA derivatives bearing an acetophenone sensitizing group, give similar values of $\Phi^{Eu} \approx 0.08$–0.09,[24] in agreement with a rather efficient metal-centred emission in Eu**P^{12}**. Finally, the sensitization efficiency is evaluated according to eqn (1): η_{sens} = 0.017. The low quantum yield determined experimentally (Φ_{tot}^{Eu} = 1.5 × 10^{-3}) is therefore mainly assigned to an inefficient sensitization process, which is expected with Trp as a Eu-sensitizer due to competitive quenching of the S1 Trp excited state by photoinduced electron transfer as explained above.

The energy transfer efficiency is highly dependent on the donor–acceptor distance with a $1/r^6$ relationship. The distance for 50% efficiency of intramolecular energy transfer by a dipole–dipole mechanism – also called the Förster distance – lies close to 3.5 Å for Tb^{3+} sensitization by Trp.[20,27] Thus, the energy transfer dramatically decreases when the donor–acceptor distance becomes greater than 3.5 Å. This steep dependence of the energy transfer on the donor–acceptor distance was indeed demonstrated experimentally with a series of octadentate ligands bearing a phenanthridinium chromophore at various distances from the emitting Ln^{3+} ion.[28] The distances between the Trp indole sensitizer and the accepting Ln^{3+} ion are 5.7 Å in Ln**P^{11}** and 8.7 Å in La**P^{22}** according to the NMR structures of these complexes.[12,13] They may be compared to the 7 Å distance measured in the X-ray structure of the Tb^{3+}-LBT developed by B. Imperiali.[11] Since the aromatic indole group is not directly coordinated to the metal, these distances are significantly longer than the Förster distance and therefore the energy transfer is clearly the limiting parameter in the quantum yields of Tb^{3+} complexes. Even though the energy transfer from Trp to Tb^{3+} is not very efficient, the latter ion is significantly sensitized upon binding to the peptides as previously described in other Ln-binding peptides or proteins.[10,11,20,29]

Europium lifetimes and CH deactivation. It has been shown that CH oscillators close to the metal ion can quench europium luminescence due to high-energy vibrational CH modes of the ligand itself.[30] A contribution of +45 s^{-1} has been evaluated for the luminescence quenching due to a proton located 3.75 Å away from the Eu centre.[21] This effect could explain the significant differences observed in the europium lifetimes measured in D_2O in the four complexes. Indeed Eu**P^{21}** and Eu**P^{22}** have quite large τ_{D2O} values around 2 ms, whereas Eu**P^{12}** and Eu**P^{11}** display significantly lower τ_{D2O} values 1.34–1.54 ms. This indicates that a quenching mechanism is present in the two latter complexes due to non exchangeable CH protons of the ligand. The examination of the solution structures previously determined for La**P^{22}** and Lu**P^{11}** shows that the S-shape of the backbone in Lu**P^{11}** due to the coordination of one amide carbonyl (Ada_1(2)) locates the Hα proton of Ada_1(5) very close to the Ln^{3+} ion (*ca* 2.8 Å). On the contrary, the U-shape structure of La**P^{22}** moves the two Hα of the Ada_2 residues far away from the cation (*ca* 6 Å). The environments of the Ln^{3+} ion in the two complexes are very similar except the Hα proton of Ada_1(5), therefore the

difference in the CH contribution to Eu luminescence quenching between the two complexes may be tentatively assigned to the close proximity of Hα(Ada$_1$(5)) and the metal centre in Eu**P^{11}**. Considering that the energy transfer is inversely proportional to the distance between the two centres in a $1/r^6$ relationship like in the general energy transfer formula developed by Förster,[31] this difference is expected to be $45\times(3.75/2.8)^6 \approx 260$ s^{-1}. This value is in very good accordance with the experimental difference calculated between the two complexes, *i.e.* $\tau_{D2O}{}^{-1}$(Eu**P^{11}**) − $\tau_{D2O}{}^{-1}$(Eu**P^{22}**) = 277 s^{-1}. Therefore, the shortening of the τ_{D2O} value observed for Eu**P^{11}** and Eu**P^{12}** with respect to Eu**P^{22}** and Eu**P^{21}** can reasonably be assigned to the presence of the proton Hα Ada$_n$(5) at a short distance to the metal centre, which deactivates Eu luminescence. The smaller CH deactivation evidenced with Eu**P^{12}** ($\tau_{D2O}{}^{-1}$ = 649 s^{-1}) with respect to Eu**P^{11}** ($\tau_{D2O}{}^{-1}$ = 746 s^{-1}) may be attributed to the higher compacity of the latter complex, which incorporates two unnatural amino acids Ada$_1$ with very short chelating side chains. This effect together with the Ln hydration numbers is in accordance with similar U-shape structures for Ln**P^{22}** and Ln**P^{21}** complexes with triply hydrated Ln^{3+} and similar S-shape structures for Ln**P^{11}** and Ln**P^{12}** with dehydrated Ln^{3+} (q = 0–1) due to coordination of the backbone carbonyl in position 2.

Structural interpretation. The photophysical properties of Ln**P^{12}** and Ln**P^{21}** compared with Ln**P^{11}** and Ln**P^{22}** allow us to predict the solution structures of these complexes, although we could not obtain satisfactory data for NMR structure computation. Indeed, the ^{1}H NMR spectra of Lu**P^{12}** and La**P^{21}** (Tables S4–5†) are indicative of only one complex in solution, but 2D NOESY or ROESY spectra did not give enough through space correlations to calculate the structures of the latter species. However, the photophysical properties of Ln**P^{21}** and Ln**P^{22}** complexes point to similar structures with a triply hydrated Ln^{3+} ion and a U-shape conformation of the peptide backbone like in the NMR structure of La**P^{22}**.[12] Indeed, both Ln complexes show a metal hydration state of 3 and an increase of Trp fluorescence upon Tb binding, which indicate a similar Trp environment in the structures. On the contrary, Ln**P^{12}** and Ln**P^{11}** complexes exhibit dehydrated Ln^{3+} ions, a decrease of Trp fluorescence upon Tb binding and short Eu luminescence lifetimes in D_2O, indicative of deactivation by CH groups of the ligand. All these characteristics allow us to conclude to the coordination of the carbonyl group of Ada$_1$(2) inducing a S-shape conformation of the peptide backbone, as evidenced previously in the NMR structure of Lu**P^{11}**.[13]

Conclusions

A series of peptides incorporating two unnatural aminoacids with aminodiacetate chelating groups Ada$_n$ (n = 1,2) was studied to rationalize the impact of the sequence on the properties of Ln complexes, *i.e.* metal hydration state, coordination numbers and peptide structure in the complex. The analysis of the Ln complexes reveals that the side-chain lengths of the Ada$_n$ moieties and their positions in the peptide sequence have dramatic effects on the properties and structures of the complexes. Indeed whereas Ada$_2$ acts as a tridentate donor, Ada$_1$ may act either as a tri- or tetradentate donor thanks to the facultative coordination of the amide carbonyl function assisted by the formation of a six-membered chelate ring. We demonstrated previously that **P^{11}** behaves as a Ln heptadentate ligand, with the carbonyl function of Ada$_1$(2) coordinated to the metal ion. This induces a dehydration of the Ln ion, which has better luminescence properties as well as an S-shape conformation of the peptide backbone preventing the formation of a β-turn. Moreover, as Ada$_1$ may act as a tetradentate donor, **P^{11}** gives binuclear complexes in excess of metal, in which the two Ada$_1$ moieties act independently.

In this paper, we investigated two novel hexapeptides **P^{12}** and **P^{21}**, which incorporate one Ada$_1$ and one Ada$_2$ in positions 2 and 5—*i.e.* on either side of the PG spacer—to rationalize the effect of Ada$_1$ position in the peptide sequence on the complexation properties. We demonstrated that Ada$_1$ acts as a tetradentate donor only in **P^{12}**—*i.e.* if placed in position 2 in the sequence. Indeed, **P^{21}** does not promote the coordination of the Ada$_1$ carbonyl group and forms a mononuclear complex with a triply hydrated Ln^{3+} ion, which transforms into polymetallic adducts in excess of metal. The examination of the luminescence properties of the series of Tb and Eu complexes indicates that Ln**P^{21}** and Ln**P^{22}** have similar structures, assigned to a U-shape complex as determined previously by solution NMR for La**P^{22}**. On the contrary, **P^{12}** gives a well-defined speciation with the formation of a unique highly dehydrated mononuclear complex (q_{Tb} = 0.2), which does not evolve into polymetallic species in excess of metal. So, when Ada$_1$ is introduced in position 2 in the peptide sequence (**P^{12}** and **P^{11}**) its carbonyl amide function is involved in the coordination of the Ln^{3+} ion instead of forming a H-bond in a β-turn like for Ada$_2$, which induces an S-shape structure like in Lu**P^{11}**. These results highlight the determination of the global shape of the complex through a single-site backbone complexation.

The stability constants $\log\beta_{110} \sim 11$ (Tb**P^{11}** and Tb**P^{12}**) have smaller values than $\log\beta_{110}$ measured for **P^{22}**, which indicates that the coordination of an extra donor—*i.e.* the carbonyl group of Ada$_1$(2)—does not stabilize the mononuclear Tb^{3+} complex. This may be explained by the metal dehydration contributions associated to the coordination of a neutral amide donor group[32] and also by the absence of the H-bond which is present in the β-turn of Tb**P^{22}**. Interestingly at physiological pH, Tb**P^{11}** and Tb**P^{12}** complexes display higher stabilities than Tb**P^{22}** due to their lower overall basicity thanks to the electron-withdrawing effect of the peptide chain.

In summary, **P^{12}** is very promising as it shows an intermediate behaviour between the two hexapeptides **P^{22}** and **P^{11}**: a simple speciation with the formation of a well-defined mononuclear complex having the luminescence and structural properties of Ln**P^{11}**. Its insertion in a more sophisticated framework for the molecular recognition of biomolecules is now considered.

Experimental

General remarks

Reagents and solvents were purchased from Aldrich and Novabiochem and used without further purification unless specified. Organic products were characterized by NMR using a Varian Mercury 400 MHz spectrometer at 298 K. Analytical and preparative peptide RP-HPLC were performed with LaChrom and LaPrep systems (see below for details).

Abbreviations. Ac_2O (acetic anhydride), AcOEt (ethyl acetate), $AcONH_4$ (ammonium acetate), Ar (aromatic), Bn (benzyl), Bu (butyl), Boc (*tert*-butyloxycarbonyl), CbzCl (benzyl chloroformate), DMAP (4-dimethylaminopyridine), DMF (*N*,*N*-dimethylformamide), DIEA (*N*,*N*-diisopropylethylamine), Dpr (L-diaminopropionic acid), DTT (dithiothreitol); Et_2O (diethyl ether), EtOH (ethanol), Fmoc (9-fluorenyl-methyloxycarbonyl), PyBOP [(benzotriazole-1-yloxy)tris(pyrrolidino) phosphonium hexafluorophosphate], *t*Bu (*tert*-butyl), TFA (trifluoroacetic acid), TIS (triisopropylsilane), TNBS (2,4,6-trinitrobenzenesulfonic acid).

Synthesis of Fmoc-Ada$_1$-(*t*Bu)$_2$-OH

Fmoc-Dpr(Boc)-OBn (2). A solution of compound **1** (1.500 g, 3.52 mmol, 1 eq) in CH_2Cl_2 (40 mL) was treated with DIEA (920 µL, 682.4 mg, 5.28 mmol, 1.5 eq) and DMAP (43.0 mg, 0.352 mmol, 0.1 eq). The resulting mixture was cooled at 0 °C and a solution of CbzCl (545 µL, 660.5 mg, 3.88 mmol, 1.1 eq) in CH_2Cl_2 (10 mL) was added dropwise over 15 min. After 3.5 h stirring at 0 °C, TLC analysis (CH_2Cl_2/AcOEt v/v = 9/1) indicated complete conversion. The mixture was washed twice with 20 mL of 5% $KHSO_4$ and dried over Na_2SO_4. After filtration and removal of the solvents *in vacuo*, purification by silica-gel column chromatography (CH_2Cl_2/AcOEt v/v = 9/1) afforded **2** in 82% yield (1.494 g). ^{1}H NMR (500 MHz, $CDCl_3$, 298 K): δ (ppm) = 7.79 (2H, d, ^3J(H,H) = 7.5 Hz, Ar); 7.63 (2H, d, ^3J(H,H) = 7.2 Hz, Ar); 7.45–7.32 (9H, m, Ar); 6.01 (1H, d, ^3J(H,H) = 6.3 Hz, NH(Fmoc)); 5.24, 5.21 (2H, AB system, J_{AB} = 12.4 Hz, CH_2(Bn)); 4.81 (1H, m, NH(Boc)); 4.48 (1H, m, Hα); 4.45–4.36 (2H, m, CH_2(Fmoc)); 4.25 (1H, m, C*H*(Fmoc)); 3.60 (2H, m, Hβ); 1.47 (9H, s, *t*Bu). ^{13}C NMR (125 MHz, $CDCl_3$, 298 K): δ (ppm) = 170.8 (*C*OOBn); 156.5 (*C*O(Fmoc)); 144.3, 144.2, 141.7 (2C) (C_q(Fmoc)); 135.6 (C_q(Bn)); 129.1, 129.0, 128.8, (C_{Ar}-H (Bn)); 128.1, 127.5, 125.6, 120.4 (C_{Ar}-H-(Fmoc)); 80.5 (C_q (*t*Bu)); 68.0 (*C*H_2(Bn)); 67.6 (*C*H_2(Fmoc)); 55.6 (*C*α); 47.6 (*C*H(Fmoc)); 42.6 (*C*β); 28.7 (*t*Bu). ES$^+$-MS ($AcONH_4$, pH = 7.0): *m*/*z* = 516.8 $[M+H]^+$.

Fmoc-Ada$_1$(*t*Bu)$_2$-OBn (3). A solution of compound **2** (1.383 g, 2.61 mmol) in TFA/CH_2Cl_2 (70 mL, v/v = 1/2) was stirred for 2 h at room temperature. The progress of Boc deprotection was monitored by TLC analysis (CH_2Cl_2/AcOEt v/v = 9/1). When the reaction was finished, solvents were removed *in vacuo* and excess TFA was discarded by azeotropic evaporation with H_2O (3 × 20 mL), EtOH (2 × 20 mL) and $CHCl_3$ (2 × 20 mL). The ES-MS analysis of the resulted solid shows the molecular peak belonging to Fmoc-Dpr-OBn (*m*/*z* = 417.2 $[M+H]^+$). The solid was dissolved in DMF (15 mL) and *tert*-butyl bromoacetate (848 µL, 1.120 g, 5.74 mmol, 2.2 eq), $KHCO_3$ (2.613 g, 26.1 mmol, 10 eq) and NBu_4I (964 mg, 2.61 mmol, 1 eq) were added. The reaction mixture was stirred for 4 h at 0 °C, and then an extra equivalent of *tert*-butyl bromoacetate was added. After an additional 2 h at 0 °C, water (60 mL) and diethyl ether (60 mL) were added to the solution. The phases were separated and the product was further extracted with diethyl ether (3 × 50 mL). The combined organic phases were washed with saturated $Na_2S_2O_3$ (50 mL), water (50 mL) and dried over Na_2SO_4. After filtration and removal of the solvents *in vacuo*, the resulting product was purified by silica-gel column chromatography (elution gradient: toluene to toluene/ether, v/v = 9/1) to yield **3** (720 mg, 43% yield) as a colorless oil. ^{1}H NMR (500 MHz, $CDCl_3$, 298 K): δ (ppm) = 7.80 (2H, d, ^3J(H,H) = 7.3 Hz, Ar); 7.75 (2H, t, ^3J(H,H) = 8.3 Hz, Ar); 7.43 (2H, t, ^3J(H,H) = 7.3 Hz, Ar); 7.45–7.28 (6H, m, Ar); 7.21 (1H, d, ^3J(H,H) = 7.0 Hz, NH(Fmoc)); 5.25, 5.21 (2H, AB system, J_{AB} = 12.4 Hz, CH_2(Bn)); 4.47 (1H, dd, $^3J_1$(H,H) = 9.2 Hz, $^3J_2$(H,H) = 6.4 Hz, CH_2(Fmoc)[a]); 4.37 (1H, m, Hα); 4.31 (2H, m, CH_2 (Fmoc)[b] and C*H*(Fmoc); 3.48, 3.39 (4H, AB system, J_{AB} = 17.8 Hz, CH_2COO*t*Bu); 3.21 (2H, m, Hβ); 1.51 (9H, s, *t*Bu). ^{13}C NMR (125 MHz, $CDCl_3$, 298 K): δ (ppm) = 171.8 (*C*OOBn)); 171.4 (*C*OOtBu); 157.1 (*C*O(Fmoc)); 144.7, 144.4, 141.7 (2C) (C_q (Fmoc)); 135.8 (C_q(Bn)); 129.5, 129.2, 129.0 (C_{Ar}-H(Bn)); 128.0, 127.5, 125.9, 120.3 (C_{Ar}-H(Fmoc)); 82.2 (C_q(*t*Bu)); 67.5 (2C) (*C*H_2(Bn), (*C*H_2(Fmoc)); 57.1 (*C*H_2-COO*t*Bu); 55.5 (*C*β); 54.1 (*C*α)); 47.6 (*C*H(Fmoc)); 28.6 (*t*Bu). ES$^+$-MS ($AcONH_4$, pH = 7.0): *m*/*z* = 667.3 $[M+Na]^+$.

Fmoc-Ada$_1$(*t*Bu)$_2$-OH. Compound **3** (700 mg, 1.11 mmol) was dissolved in 50 mL of absolute ethanol and hydrogenated (3 bar, overnight) over 100 mg 10% Pd/C. Fmoc-Ada$_1$(*t*Bu)$_2$-OH was obtained as a hygroscopic glassy solid (568 mg, 94% yield) after filtration of the reaction mixture through a Celite pad and solvent evaporation. ^{1}H NMR (500 MHz, $CDCl_3$, 298 K): δ (ppm) = 7.79 (2H, d, ^3J(H,H) = 7.4 Hz, Ar); 7.63 (2H, d, ^3J(H,H) = 7.4 Hz, Ar); 7.43 (2H, t, ^3J(H,H) = 7.4 Hz, Ar); 7.34 (2H, t, ^3J(H,H) = 7.4 Hz, Ar); 6.06 (1H, d, ^3J(H,H) = 4 Hz, NH(Fmoc)); 4.40 (2H, m, CH_2 (Fmoc)); 4.26–4.20 (2H, m, C*H* (Fmoc) and Hα); 3.59, 3.51 (4H, AB system, J_{AB} = 18.0 Hz, CH_2COOtBu); 3.48 (1H, m, Hβ[a]); 2.79 (1H, m, Hβ[b]); 1.51 (18H, s, *t*Bu). ^{13}C NMR (125 MHz, $CDCl_3$, 298 K): δ (ppm) = 172.4 (*C*OOH); 171.1(*C*OOtBu); 156.5 (*C*O (Fmoc)); 144.2, 144.1, 141.7 (2C) (C_q (Fmoc)); 128.2, 127.5, 125.6, 120.4 (C_{Ar}-H (Fmoc)); 83.1(C_q (*t*Bu)); 67.7 (*C*H_2 (Fmoc)); 57.7 (*C*H_2COOtBu); 57.4 (*C*β); 51.9 (*C*α); 47.5 (*C*H (Fmoc)); 28.5 (*t*Bu). ES$^+$-MS ($AcONH_4$, pH = 7.0): *m*/*z* = 577.3 $[M+Na]^+$; elemental analysis calcd (%) for $C_{30}H_8N_2O_8$.1.5 H_2O: C 61.95, H 7.10, N 4.82; found: C 61.64, H 6.87, N 4.87.

Control of Fmoc-Ada$_1$(*t*Bu)$_2$-OH enantiopurity by ^{1}H NMR. A solution of Fmoc-Ada$_1$(*t*Bu)$_2$-OH (30 mg, 54 µmol) and α-methylbenzylamine (14 µL, 13.3 mg, 110 µmol, 2 eq, either in enantiopure (*S*) or in racemic form) in 0.5 mL of CH_2Cl_2 was treated with PyBOP (54 mg, 104 µmol, 2 eq), DIEA (57 µL, 42 mg, 327 µmol, 6 eq) and stirred for 3 h. The resulting mixture of products was separated by silica-gel column chromatography (CH_2Cl_2/AcOEt v/v = 15/85) and each fraction was identified by 1D ^{1}H NMR. In the spectra of the adducts, a splitting of the NH amide resonances was detected only for the coupling products with the racemic amine. This indicates that no racemization of Fmoc-Ada$_1$(*t*Bu)$_2$-OH occurred during the synthesis (assuming that 2% diastereomeric product would be detected by NMR, *ee* > 96%).

Peptide synthesis

The hexapeptides were assembled manually by solid-phase peptide synthesis on Rink Amide MBHA resin (substitution

0.59 mmol g^{-1}, 150 mg) using Fmoc chemistry. The synthesis was started by an initial deprotection of the commercially resin-bound Fmoc with DMF/piperidine (v/v = 4/1). Couplings were performed with N^{α}-Fmoc-protected amino acids (2 equiv.), PyBOP (2 equiv.), and DIEA (6 equiv.) in DMF for 30 min. In the case of Fmoc-Ada$_n$(tBu)$_2$-OH the coupling reaction was monitored by a TNBS test.[33] For incomplete reactions, a second coupling with Fmoc-Ada$_n$(tBu)$_2$-OH (0.5 equiv.) PyBOP (1 equiv.), and DIEA (4 equiv.) was performed. After each coupling, the resin was treated with DMF/pyridine/Ac_2O (v/v/v = 7/2/1) to acetylate unreacted amino groups (2 × 2 min). Fmoc deprotection was achieved with DMF/piperidine (v/v = 4/1) (3 × 3 min). The yield of each peptide coupling was monitored by UV-Vis spectroscopy (ε_{300} = 7800 L mol^{-1} cm^{-1} for the piperidine adduct of dibenzofulvene). After the final Fmoc deprotection, the peptide was acetylated as described above. The peptide was freed from the resin and the side-chain protections were removed by treatment with a cleavage cocktail consisting of 200 mg DTT dissolved in 20 mL TFA/TIS/H_2O (v/v/v = 92/4/4). After 2.5 h of stirring, the solution was evaporated to yield a yellow oil, which was triturated in Et_2O until a white powder was obtained. This solid was analysed C18 Reverse Phase HPLC [Merck Purospher® STAR endcapped, 4.6 × 250 mm, 5 μm particles, solvent A = H_2O/TFA (v/v = 99.925/0.075), solvent B = CH_3CN/H_2O/TFA (v/v/v = 90/10/0.1), elution gradient: from v_A/v_B = 1/9 to v_A/v_B = 4/6 in 15 min, flow rate 1 mL min^{-1}, UV monitoring at 280 nm]. HPLC analysis indicated that the solid consists essentially of one product. The solid residue was dissolved in water/acetonitrile (v/v = 9/1) and easily purified by C18 reversed-phase high-performance liquid chromatography [RP-HPLC, Merck Purospher®, 250 × 40 mm, 10 μm C_{18} particles, solvent A = H_2O/TFA (v/v = 99.925/0.075), solvent B = CH_3CN/H_2O/TFA (v/v/v = 90/10/0.1), elution gradient: from 10 v_A/v_B = 1/9 to v_A/v_B = 4/6 in 15 min, flow rate 75 mL min^{-1}] to yield the desired peptide as a white powder.

P^{11}: Ac-WAda$_1$PGAda$_1$G-NH_2, Yield of the on-resin synthesis (UV): 76%, Isolated mass: 44.5 mg (isolated yield assuming that the solid is **P^{11}**·2TFA: 45%). ES^+ MS ($AcONH_4$, pH 7): m/z = 861.2 $[M+H]^+$, ES^--MS ($AcONH_4$, pH = 7.0): m/z = 859.2 $[M-H]^-$; RP-HPLC: t_R = 10.8 min, >95% purity (NMR).

P^{12}: Ac-WAda$_1$PGAda$_2$G-NH_2, Yield of the on-resin synthesis (UV): 60%, Isolated mass: 40.5 mg (isolated yield assuming that the solid is **P^{12}**·2TFA: 36%). ES^+-MS ($AcONH_4$, pH 7): m/z = 875.3 $[M+H]^+$, ES^--MS ($AcONH_4$, pH = 7.0): m/z = 873.3 $[M-H]^-$; RP-HPLC: t_R = 11.0 min, >95% purity (NMR).

P^{21}: Ac-Wada$_2$PGAda$_1$G-NH_2, Yield of the on-resin synthesis (UV): 82%, Isolated mass: 54 mg (isolated yield assuming that the solid is **P^{21}**·2TFA: 48%). ES^+-MS ($AcONH_4$, pH 7.0): m/z = 875.3 $[M+H]^+$, ES^--MS ($AcONH_4$, pH = 7.0): m/z = 873.3 $[M-H]^-$; RP-HPLC: t_R = 10.9 min, >95% purity (NMR).

pH-metric titration

Continuous potentiometric titrations with 0.1 M KOH were conducted in 5 mL aqueous solutions of peptide (0.5 mM) with KCl (0.1 M) as background electrolyte. The reverse titrations with 0.1 M HCl were performed after each experiment to check whether equilibration had been achieved. In a typical experiment, 90 points (2 μL increment) were measured with a 2 min delay between the measurements. Experimental data were refined using the computer program Hyperquad 2000.[34] All equilibrium constants were expressed as concentration rather than activity ratios. The ionic product of water at 25 °C and 0.1 M ionic strength was pK_w = 13.78.[35] The initial concentration of the ligand was determined by UV-vis spectroscopy (ε_{280} = 5690 L mol^{-1} cm^{-1} for tryptophan residues), and proton content was adjusted to fit the observed values (since the peptides are present in the lyophilised solid as a mixture of protonation states, the proton content was reproducible for a given peptide). All values and errors (one standard deviation) reported represent the average of three independent experiments.

Preparation of aqueous solutions

The 3 mM and 30 mM aqueous solutions of lanthanides were prepared by dissolving corresponding salts ($TbCl_3·6H_2O$, $Tb(OTf)_3$, $EuCl_3·6H_2O$, $LuCl_3·6H_2O$ and $LaCl_3·7H_2O$) in deionized water. The precise concentrations were determined by colorimetric titration with 5mM EDTA (Fisher Chemicals) in the presence of xylenol orange indicator. Peptide solutions in HEPES buffer (10 mM, 0.1 M KCl, pH = 7.0) were prepared directly before the use. The precise concentrations were established by UV absorption at 280 nm using the known extinction coefficient of tryptophan (ε_{280} = 5690 L mol^{-1} cm^{-1}). HEPES buffer (10 mM, 0.1 M KCl, pH = 7.0) was prepared from solid 4-(2-hydroxyethyl)-piperazine-1-ethanesulfonic acid (Fluka) and potassium chloride in deionized H_2O (or D_2O). The pH (or pD) was adjusted to 7.0 with KOH (or NaOD).

Electrospray mass spectrometry of Eu**P$^{nn'}$** complexes

The mass spectrometry measurements were performed with a LXQ-type Thermo Scientific spectrometer equipped with an electrospray ionization source and a linear trap detector. The samples of Eu**P$^{nn'}$** complexes were prepared by adding $EuCl_3$ (0, 0.5, 1.0, 2.0 equiv.) to a peptide solution (60 μM) in $AcONH_4$ buffer (20 mM, pH = 7.0). Resulting mixtures where injected into the spectrometer at a flow rate of 5 μL min^{-1}. 2kV voltage and 250 °C capillary temperature were applied.

Circular dichroism measurements

The CD spectra were collected on an Applied Photophysics Chirascan spectrometer in a 1 cm path length quartz cell at 25 °C. The 20 μM solutions of free peptides and Tb-peptide complexes (0.5, 1, 1.5, 2 equiv. of $Tb(OTf)_3$) were prepared in deionized water and the pH was adjusted to 7.0 with KOH. Subsequently, the CD measurements were performed in 280–200 nm range with a 1 nm interval, 2 s time constant, 1 nm bandwidth and three scans. The CD signal was reported in molar ellipticity per α-amino acid residue ($[\theta]$ in units of deg cm^2 mol^{-1}; $[\theta] = \theta_{obs}/(10lcn)$, with θ_{obs} the observed ellipticity in m°, l the optical path length of the cell in cm, c the peptide concentration in mol L^{-1}, and n the number of residues in the peptide (n = 6 in this case)).

Luminescence measurements

The luminescence measurements were performed on a LS50B spectrofluorimeter connected to a computer equipped with

FLWINLAB 2.0. The spectra were recorded in a 1 cm path length quartz luminescence cell at 25 °C, by exciting the sample at 280 nm and recording the emission with maximum at 350 nm (tryptophan fluorescence), 545 nm (Tb-centred luminescence) or 618 nm (Eu-centred luminescence). For fluorescence measurements, excitation slit: 3.0 nm and emission slit: 8.0 nm were applied. The terbium and europium emission spectra were recorded after 0.05 ms delay, with gate time/excitation slit/emission slit: 1 ms/10 nm/5 nm and 0.5 ms/10 nm/15 nm for Tb^{3+} and Eu^{3+}, respectively. The 430 nm cut-off filter was used during all tryptophan-sensitized luminescence measurements.

The competition titrations were performed with delays chosen to maximize the differences in Tb emission intensities of the two complexes (Fig. S3–S4†). The experimental data were fitted with fixed values of the conditional stability constant of the reference peptide and the ratio of the luminescence intensities measured in the same conditions.

The quantum yield measurements were performed according to Chauvin *et al.*[23] in a 1 cm path length luminescence cell at 25 °C on aqueous solutions of Tb**P**$^{\mathbf{nn'}}$, Eu**P**$^{\mathbf{nn'}}$(50 μM, A_{280} = 0.3), $[Tb(dpa)_3]^{3-}$ (0.107 mM, A_{280} = 0.295) and $[Eu(dpa)_3]^{3-}$ (0.110 mM, A_{280} = 0.295) in HEPES buffer (10 mM, 0.1 M KCl, pH = 7.0). The standard solutions of $[Tb(dpa)_3]^{3-}$ and $[Eu(dpa)_3]^{3-}$ were prepared by mixing Tb^{3+}/Eu^{3+} with dipicolinic acid (dpa) in 1/3 equivalent ratio in HEPES buffer (10 mM, 0.1 M KCl, pH = 7.0) and stirring the resulting mixture during 5 min. The quantum yields Φ have been calculated using the equation $\Phi_x/\Phi_r = (E_x/E_r) \times (A_r(\lambda_r)/A_x(\lambda_x))$, where x refers to the sample and r to the reference; E is the integrated luminescence intensity and A is the absorbance of the solution at the excitation wavelength λ. The values of quantum yields Φ_{dpa}^{Tb} = 18.4 ± 2.5% (0.107 mM, A_{280} = 0.295) and Φ_{dpa}^{Eu} = 20.4 ± 2.5% (0.110 mM, A_{280} = 0.295) were applied to the calculations assuming that the change of a buffer from Tris (0.1 M, pH = 7.45) to HEPES (10 mM, 0.1 M KCl, pH = 7.0) has affected the reference values in the error range.[23]

Acknowledgements

The authors wish to thank Dr Daniel Imbert and Dr Graeme Stasiuk for constructive discussions and experimental assistance and Yves Chenavier for the synthesis of the unnatural amino acids.

Notes and references

1 O. Seneque, S. Crouzy, D. Boturyn, P. Dumy, M. Ferrand and P. Delangle, *Chem. Commun.*, 2004, 770; E. Rossy, O. Seneque, D. Lascoux, D. Lemaire, S. Crouzy, P. Delangle and J. Coves, *FEBS Lett.*, 2004, **575**, 86; P. Rousselot-Pailley, O. Seneque, C. Lebrun, S. Crouzy, D. Boturyn, P. Dumy, M. Ferrand and P. Delangle, *Inorg. Chem.*, 2006, **45**, 5510; S. J. Opella, T. M. DeSilva and G. Veglia, *Curr. Opin. Chem. Biol.*, 2002, **6**, 217; G. Veglia, F. Porcelli, T. DeSilva, A. Prantner and S. J. Opella, *J. Am. Chem. Soc.*, 2000, **122**, 2389; J. Jiang, I. A. Nadas, M. A. Kim and K. J. Franz, *Inorg. Chem.*, 2005, **44**, 9787; K. J. Franz, K. L. Haas, A. B. Putterman, D. R. White and D. J. Thiele, *J. Am. Chem. Soc.*, 2011, **133**, 4427; K. J. Franz, J. T. Rubino, M. P. Chenkin, M. Keller and P. Riggs-Gelasco, *Metallomics*, 2011, **3**, 61; K. J. Franz, J. T. Rubino and P. Riggs-Gelasco, *JBIC, J. Biol. Inorg. Chem.*, 2010, **15**, 1033.

2 A. M. Pujol, C. Gateau, C. Lebrun and P. Delangle, *J. Am. Chem. Soc.*, 2009, **131**, 6928; A. M. Pujol, M. Cuillel, O. Renaudet, C. Lebrun, P. Charbonnier, D. Cassio, C. Gateau, P. Dumy, E. Mintz and P. Delangle, *J. Am. Chem. Soc.*, 2011, **133**, 286; A. M. Pujol, C. Gateau, C. Lebrun and P. Delangle, *Chem.–Eur. J.*, 2011, **17**, 4418.

3 K. N. Allen and B. Imperiali, *Curr. Opin. Chem. Biol.*, 2010, **14**, 247.

4 C. S. Bonnet, P. H. Fries, S. Crouzy, O. Sénèque, F. Cisnetti, D. Boturyn, P. Dumy and P. Delangle, *Chem.–Eur. J.*, 2009, **15**, 7083; C. S. Bonnet, P. H. Fries, S. Crouzy and P. Delangle, *J. Phys. Chem. B*, 2010, **114**, 8770.

5 J.-C. G. Bünzli, *Acc. Chem. Res.*, 2006, **39**, 53; D. Parker, *Chem. Soc. Rev.*, 2004, **33**, 156; J.-C. Bünzli and C. Piguet, *Chem. Soc. Rev.*, 2005, **34**, 1048.

6 P. Caravan, J. J. Ellison, T. J. McMurry and R. B. Lauffer, *Chem. Rev.*, 1999, **99**, 2293; S. Aime, S. G. Crich, E. Gianolio, G. B. Giovenzana, L. Tei and E. Terreno, *Coord. Chem. Rev.*, 2006, **250**, 1562.

7 J. C. G. Bunzli and S. V. Eliseeva, *Chem. Soc. Rev.*, 2010, **39**, 189; J.-C. G. Bünzli, *Chem. Lett.*, 2009, **38**, 104; D. Parker, E. J. New, D. G. Smith and J. W. Walton, *Curr. Opin. Chem. Biol.*, 2010, **14**, 238.

8 C. W. Hogue, J. P. MacManus, D. Banville and A. G. Szabo, *J. Biol. Chem.*, 1992, **267**, 13340; P. Caravan, J. M. Greenwood, J. T. Welch and S. Franklin, *Chem. Commun.*, 2003, 2574; S. J. Franklin, *Curr. Opin. Chem. Biol.*, 2001, **5**, 201; R. T. Kovacic, J. T. Welch and S. J. Franklin, *J. Am. Chem. Soc.*, 2003, **125**, 6656.

9 J. P. MacManus, C. W. Hogue, B. J. Marsden, M. Sikorska and A. G. Szabo, *J. Biol. Chem.*, 1990, **265**, 10358.

10 K. J. Franz, M. Nitz and B. Imperiali, *ChemBioChem*, 2003, **4**, 265; M. Nitz, K. J. Franz, R. L. Maglathlin and B. Imperiali, *ChemBioChem*, 2003, **4**, 272.

11 M. Nitz, M. Sherawat, K. J. Franz, E. Peisach, K. N. Allen and B. Imperiali, *Angew. Chem., Int. Ed.*, 2004, **43**, 3682.

12 F. Cisnetti, C. Gateau, C. Lebrun and P. Delangle, *Chem.–Eur. J.*, 2009, **15**, 7456.

13 F. Cisnetti, C. Lebrun and P. Delangle, *Dalton Trans.*, 2010, **39**, 3560.

14 A. Borics, R. F. Murphy and S. Lovas, *J. Biomol. Struct. Dyn.*, 2004, **21**, 761; S. R. Raghothama, S. K. Awasthi and P. Balaram, *J. Chem. Soc., Perkin Trans. 2*, 1998, 137.

15 W. M. Kazmierski, *Tetrahedron Lett.*, 1993, **34**, 4493; W. M. Kazmierski, *Int. J. Pept. Protein Res.*, 2009, **45**, 241.

16 O. V. Larionov and A. de Meijere, *Org. Lett.*, 2004, **6**, 2153.

17 K. Wüthrich, *NMR of Proteins and Nucleic Acids*, Wiley, New York, 1986.

18 D. Parker, *Coord. Chem. Rev.*, 2000, **205**, 109.

19 P. J. Breen, E. K. Hild and W. W. de Horrocks, *Biochemistry*, 1985, **24**, 4991; W. W. de Horrocks, J. P. Bolender, W. D. Smith and R. M. Supkowski, *J. Am. Chem. Soc.*, 1997, **119**, 5972.

20 W. W. de Horrocks and W. E. Collier, *J. Am. Chem. Soc.*, 1981, **103**, 2856.

21 A. Beeby, I. M. Clarkson, R. S. Dickins, S. Faulkner, D. Parker, L. Royle, A. S. d. Sousa, J. A. G. Williams and M. Woods, *J. Chem. Soc., Perkin Trans. 2*, 1999, 493.

22 W. W. de Horrocks and D. R. Sudnick, *J. Am. Chem. Soc.*, 1979, **101**, 334.

23 A. S. Chauvin, F. Gumy, D. Imbert and J. C. G. Bunzli, *Spectrosc. Lett.*, 2004, **37**, 517; A. S. Chauvin, F. Gumy, D. Imbert and J. C. G. Bunzli, *Spectrosc. Lett.*, 2007, **40**, 193.

24 A. Beeby, L. M. Bushby, D. Maffeo and J. A. G. Williams, *J. Chem. Soc., Dalton Trans.*, 2002, 48.

25 M. H. V. Werts, R. T. F. Jukes and J. W. Verhoeven, *Phys. Chem. Chem. Phys.*, 2002, **4**, 1542.

26 C. Piguet, J. M. Senegas, G. Bernardinelli, D. Imbert, J. C. G. Bunzli, P. Y. Morgantini and J. Weber, *Inorg. Chem.*, 2003, **42**, 4680.

27 L. S. McNemar, W. Y. Lin, C. D. Eads, W. M. Atkins, P. Dombrosky and J. J. Villafranca, *Biochemistry*, 1991, **30**, 3417.

28 I. M. Clarkson, A. Beeby, J. I. Bruce, L. J. Govenlock, M. P. Lowe, C. E. Mathieu, D. Parker and K. Senanayake, *New J. Chem.*, 2000, **24**, 377.

29 B. D. Schlyer, D. G. Steel and A. Gafni, *J. Biol. Chem.*, 1995, **270**, 22890.

30 R. S. Dickins, D. Parker, A. S. deSousa and J. A. G. Williams, *Chem. Commun.*, 1996, 697.

31 T. Forster, *Ann. Phys.*, 1948, **437**, 55.

32 F. Bravard, C. Rosset and P. Delangle, *Dalton Trans.*, 2004, 2012.

33 W. S. Hancock and J. E. Battersby, *Anal. Biochem.*, 1976, **71**, 260.

34 P. Gans, A. Sabatini and A. Vacca, *Talanta*, 1996, **43**, 1739.

35 R. M. Smith, A. E. Martell and R. J. Motekaitis, NIST Critically Selected Stability Constants of Metal Complexes Database, NIST Standard Reference Database 46, 2001.